The theoretical temperature-pressure phase diagram for betaine calcium chloride dihydrate (BCCD)

1998 J. Phys.: Condens. Matter 10 1803

(http://iopscience.iop.org/0953-8984/10/8/013)

J. Phys.: Condens. Matter **10** (1998) 1803–1812. Printed in the UK PII: S0953-8984(98)84796-6

The theoretical temperature–pressure phase diagram for betaine calcium chloride dihydrate (BCCD)

D G Sannikov† and G Schaack

Physikalisches Institut der Universität Würzburg, Am Hubland, 97074 Würzburg, Germany

Received 30 May 1997, in final form 24 October 1997

Abstract. Theoretical phase diagrams for betaine calcium chloride dihydrate are constructed. A phenomenological approach is used. Expressions for the thermodynamic potentials of different phases and for the boundaries between these phases are given in an explicit form. The theoretical temperature–pressure phase diagram is plotted and is found to be in agreement with the experimental diagram. The approximations and assumptions made in the construction of the diagrams are discussed.

1. Introduction

Betaine calcium chloride dihydrate (BCCD), $(CH_3)_3NCH_2COO{\cdot}CaCl_2{\cdot}2H_2O$, is a well studied crystal with an incommensurate phase (IC phase). The number of observed commensurate phases ($C_{m/l}$ phases, with different values of the dimensionless wavenumber $q = q_{m/l} = m/l$) is very large. The experimental temperature–pressure (T–P) phase diagram, which was obtained by means of dielectric measurements [1–4], is shown schematically in figure 1.

The phase diagram has also been investigated by ultrasound techniques over a restricted range of T and P in [5]. On the basis of a study of elastic neutron scattering in partially deuterated BCCD, a P–T diagram has been plotted [6]. Both of these latter diagrams are closely related to the diagram shown in figure 1.

The space group D_{2h}^{16} of the initial C phase is usually chosen in the standard setting abc, i.e. $Pnma$. The vector of modulation of the IC phase is $k_z = qc^*$. The following $C_{m/l}$ phases are observed in figure 1: the $C_{0/1}$ phase with $q = 0$ (i.e. equitranslational with the C phase), which has a spontaneous polarization along the y-axis (its space group is C_{2v}^9 ($Pn2_1a$)); and $C_{m/l}$ phases with $q_{m/l} = m/l = 2/7, 1/4, 1/5, 1/6, 1/7$ and other $q_{m/l}$ which are not labelled in figure 1 (see [1–4] and references therein). Possible space groups of the $C_{m/l}$ phases are given below in table 1.

The aim of this paper is to construct theoretical phase diagrams for BCCD on the basis of a phenomenological approach. First we construct a phase diagram in dimensionless variables D and A, which are combinations of coefficients of thermodynamic potentials (see below). Assuming a linear dependence of D and A on T and P, we construct the T–P phase diagram and compare it with the experimental diagram.

† Permanent address: Shubnikov Institute of Crystallography of the Russian Academy of Sciences, Moscow 117333, Russia.

0953-8984/98/081803+10$19.50

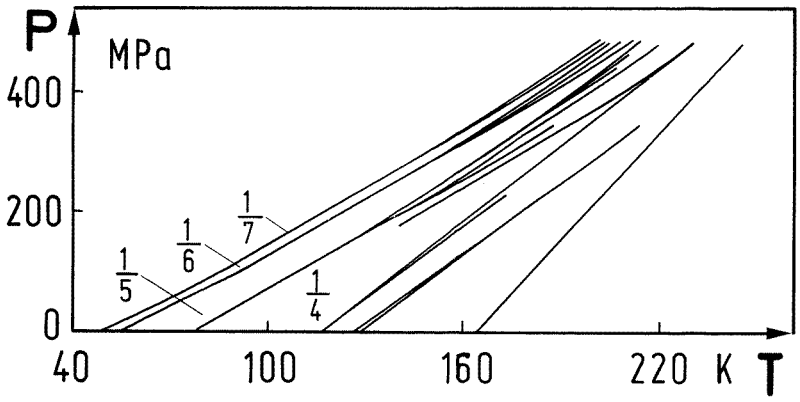

Figure 1. The experimental T–P phase diagram for BCCD [1–4].

2. Thermodynamic potentials

We assume, as is indeed the case, that all of the phases observed in BCCD are determined by the same soft optical branch of the normal vibration spectrum of the crystal (the language of lattice dynamics is useful for the cases of displacive phase transitions and order–disorder ones).

The first problem is that of obtaining the thermodynamic potentials for all of the possible phases in BCCD. For this purpose we combine two different phenomenological approaches to the description of IC phase transitions. Having in mind further developments of the theory, we write the potentials out taking into consideration all external forces which can influence the $C_{m/l}$ phases and hence the phase diagrams substantially. These external forces are various components of the electric field vector, E_i, and of the mechanical stress tensor, σ_{ij}.

In the first approach, the order parameter of the C–$C_{0/1}$ phase transition is used as an order parameter for the C–IC–$C_{0/1}$ transition sequence, except that it is dependent on space coordinates. Since the C–$C_{0/1}$ transition is a proper ferroelectric one, i.e. the nondegenerate mode of the soft optical branch in the centre of the Brillouin zone contributes to the polarization P_y, we can choose the component $P_y(z)$ as an order parameter. The thermodynamic potential then takes the form [7, 8]

$$\begin{aligned} \Phi &= \int \Phi(z)\,\mathrm{d}z \Big/ \int \mathrm{d}z \\ \Phi(z) &= \alpha P_y^2 + \frac{2}{3}\beta P_y^4 - \frac{\delta}{c^{*2}}\left(\frac{\partial P_y}{\partial z}\right)^2 + \frac{\kappa}{c^{*4}}\left(\frac{\partial^2 P_y}{\partial z^2}\right)^2 - P_y E_y. \end{aligned} \tag{2.1}$$

In a single-harmonic approximation,

$$P_y = p + \sqrt{2}\rho \cos qc^* z \tag{2.2}$$

($p = 0$ at $E_y = 0$) the potential of the IC phase according to equation (2.1) takes the form

$$\Phi_{\mathrm{IC}} = \alpha(q)\rho^2 + \beta\rho^4 + \alpha p^2 + \frac{2}{3}\beta p^4 + 4\beta\rho^2 p^2 - pE_y \tag{2.3}$$

where

$$\alpha(q) = \alpha - \delta q^2 + \kappa q^4 \tag{2.4}$$

Table 1. The space groups of all of the possible commensurate phases associated with a soft optical branch with the wavevector $k_z = qc^*$ of the space group $Pnma$ (D_{2h}^{16}) of BCCD. The mode with $q = 0$ of this branch transforms according to the representation B_{2u} of the point group D_{2h} of the initial phase of the crystal.

$q = q_{m/l} = m/l$:	0/1			m_+/l_-			m_-/l_-			m_-/l_+		
$B_{2u}(y)$	C_{2v}^9	$Pn2_1a$	c_1	C_{2v}^9	$Pn2_1a$	y	D_2^4	$P2_12_12_1$	xyz	C_{2h}^5	$P12_1/c1$	zx
			c_2	C_{2h}^5	$P2_1/n11$	yz	C_{2h}^5	$P112_1/a$	xy	C_{2v}^5	$P2_1ca$	x
			c_3	C_s^2	$Pn11$	z	C_2^2	$P112_1$	z	C_s^2	$P1c1$	z

and it is necessary to assume $\beta > 0$, $\kappa > 0$, and also $\delta > 0$.

For the potentials of the C phase and the $C_{0/1}$ phase we obtain from equation (2.1)

$$\Phi_C = \alpha P_y^2 + \frac{2}{3}\beta P_y^4 - P_y E_y. \tag{2.5}$$

It is impossible to obtain potentials for the $C_{m/l}$ phases in the first approach. Therefore we use the second approach, namely a phenomenological description of a devil's staircase [9]. The dependence of the elastic coefficient α of the soft optical branch on the wavenumber q can be approximated by the simplest function (2.4). It has a maximum in the centre and a minimum at an arbitrary point of the Brillouin zone. Since the soft optical branch is doubly degenerate, i.e. $\alpha(q) = \alpha(-q)$, the order parameter in the potential, which corresponds to an arbitrary q-value, has two components. The components η and ξ can be considered as amplitudes of two modes with wavenumbers q and $-q$, which belong to this branch. It is convenient to use the polar system of coordinates $\eta = R\cos\varphi$, $\xi = R\sin\varphi$. There exist two independent invariants composed of the components η and ξ: R^2 (isotropic) and $R^{2l}\cos 2l\varphi$ (anisotropic in the η, ξ-space). Three mixed invariants also exist in our case: $Q_1\rho^l\cos l\varphi$, $Q_2\rho^l\sin l\varphi$, and $Q_3\rho^{2l}\sin 2l\varphi$, which, along with the components η and ξ of the order parameter, contain macroscopic quantities (tensor components $Q_{1,2,3}$) in linear form. These transform according to representations of the point group D_{2h}; for details see reference [10].

Then the thermodynamic potential can be represented in the form

$$\Phi = \alpha(q)R^2 + \beta R^4 - \tilde{\alpha}'_{2l}R^{2l}\cos 2l\varphi - a_1Q_1R^l\cos l\varphi - a_2Q_2R^l\sin l\varphi \\ - a_3Q_3R^{2l}\sin 2l\varphi + \kappa_1Q_1^2 + \kappa_2Q_2^2 + \kappa_3Q_3^2 - Q_1F_1 - Q_2F_2 - Q_3F_3 \tag{2.6}$$

where F_1, F_2, and F_3 are components of the external forces conjugate to Q_1, Q_2, and Q_3. The components of the electric field vector, E_i, or the stress tensor, σ_{ij}, as well as $F_{1,2,3}$ and P_i or $u_{i,j}$ as well as $Q_{1,2,3}$ are of interest from the experimental point of view. The particular meaning of $Q_{1,2,3}$ and hence of $F_{1,2,3}$ depends on the $q = m/l$ considered, and on whether m and l are even or odd. This can be seen from table 1 [10, 11].

Table 1 gives the space groups for all possible $C_{m/l}$ phases, which correspond to the soft branch of the normal vibration spectrum of BCCD under consideration. The first column gives the representation of the point group D_{2h} (mmm), according to which the transition from the C phase to the $C_{0/1}$ phase occurs, and in parentheses the lower-rank tensor component which transforms according to this representation; finally the space group of the $C_{0/1}$ phase is given. The three columns that follow give the space groups of three possible $C_{m/l}$ phases: c_1 ($Q_1 \neq 0$), c_2 ($Q_2 \neq 0$), and c_3 ($Q_{1,2,3} \neq 0$) for all $q_{m/l} = m/l$ (m_+, l_+ are even integers and m_-, l_- are odd integers), and also lower-rank tensor components, which transform according to the same representations as Q_1, Q_2, and Q_3. Note that the phase

c_3, if it exists, occupies a small volume in the phase space in comparison with the phases c_1, c_2, and hence will be rather unlikely to be observed in experiment (see [11]).

We require that potential (2.6) leads to the same expression, equations (2.3), (2.4), for the IC phase as in the first approach. For irrational values of q the coefficients $\tilde{\alpha}'_{2l}$ and $a_{1,2,3}$ are identically equal to zero: the terms with these coefficients are not invariants, because they do not satisfy the condition of translational symmetry of the crystal along the z-axis. Setting $\tilde{\alpha}'_{2l} = a_1 = a_2 = a_3 = 0$, we obtain (2.3) and (2.4) from (2.6), if we add to (2.6) the following terms:

$$\Delta\Phi = \alpha P_y^2 + \frac{2}{3}\beta P_y^4 + 4\beta R^2 P_y^2 - P_y E_y. \tag{2.7}$$

Note that the terms $\kappa_\alpha Q_\alpha^2 - Q_\alpha F_\alpha$ ($\alpha = 1, 2, 3$) were not taken into account in (2.3), apart from the term $-P_y E_y$, and that ρ and p are changed to R and P_y in (2.6) and (2.7) in comparison with (2.3). Strictly speaking, the terms $\kappa_\alpha Q_\alpha^2 - Q_\alpha F_\alpha$ must be added to the potentials (2.3) and (2.5), while the change of variables is not essential. P_y is a uniform component of the polarization vector, as in (2.5), which is proportional to the amplitude of the mode with $q = 0$ belonging to the soft branch considered. The last term in (2.7) must be added only if it is absent among the terms $-Q_\alpha F_\alpha$ in (2.6). In (2.6) and (2.7) we take into account only the necessary invariants of the lowest powers in R and also all external forces, which are linearly dependent on the order parameter. Invariants of higher powers in R do not change the results substantially.

Thus, using two different phenomenological approaches for the description of IC phase transitions, and requiring that they must provide precisely the same expressions for the potential of the IC phase, we have obtained the thermodynamic potentials for all of the possible phases in BCCD.

3. Potentials for concrete $q_{m/l}$-values

For definiteness, we rewrite potentials (2.6) and (2.7) for each $q_{m/l} = m/l$, giving the explicit meaning for Q_1, Q_2 and F_1, F_2, and renaming some coefficients. We omit Q_3 and F_3 since the field F_3 does not influence the phase diagrams significantly.

For the C_{m_-/l_+} phases with $q_{m_-/l_+} = m_-/l_+$, we obtain

$$\begin{aligned}\Phi_{m_-/l_+} = {} & \alpha(q_{m_-/l_+})R^2 + \beta R^4 - \tilde{\alpha}'_{2l} R^{2l}\cos 2l\varphi + \alpha P_y^2 + \tfrac{2}{3}\beta P_y^4 + 4\beta R^2 P_y^2 \\ & - b_5 u_{zx} R^l \cos l\varphi - b_1 P_x R^l \sin l\varphi \\ & + c_5 u_{zx}^2 + c_1 P_x^2 - P_y E_y - u_{zx}\sigma_{zx} - P_x E_x. \end{aligned} \tag{3.1}$$

For the C_{m_-/l_-} phases with $q_{m_-/l_-} = m_-/l_-$ we get

$$\begin{aligned}\Phi_{m_-/l_-} = {} & \alpha(q_{m_-/l_-})R^2 + \beta R^4 - \tilde{\alpha}'_{2l} R^{2l}\cos 2l\varphi + \alpha P_y^2 + \tfrac{2}{3}\beta P_y^4 + 4\beta R^2 P_y^2 \\ & - b_6 u_{xy} R^l \sin l\varphi + c_6 u_{xy}^2 - P_y E_y - u_{xy}\sigma_{xy}. \end{aligned} \tag{3.2}$$

Here we omit the mixed invariants with the components $P_x u_{yz}$, $P_y u_{zx}$, and $P_z u_{xy}$, since the associated forces $E_x\sigma_{yz}$, $E_y\sigma_{zx}$, and $E_z\sigma_{xy}$ are not important from the experimental point of view.

For the C_{m_+/l_-} phases with $q_{m_+/l_-} = m_+/l_-$, we obtain

$$\begin{aligned}\Phi_{m_+/l_-} = {} & \alpha(q_{m_+/l_-})R^2 + \beta R^4 - \tilde{\alpha}'_{2l} R^{2l}\cos 2l\varphi + \alpha P_y^2 + \tfrac{2}{3}\beta P_y^4 + 4\beta R^2 P_y^2 \\ & - b_2 P_y R^l \cos l\varphi - b_4 u_{yz} R^l \sin l\varphi + c_4 u_{yz}^2 - P_y E_y - u_{yz}\sigma_{yz}. \end{aligned} \tag{3.3}$$

In (3.1)–(3.3) we have included those components of E_i and σ_{ij} which could be of interest in experimental investigations of their influence on the $C_{m/l}$ phases. However, in the present context they are not needed.

4. Equilibrium values of the potentials at zero fields

We consider the thermodynamic potentials in the absence of fields, i.e. $E_i = 0, \sigma_{ij} = 0$. Minimizing the IC phase potential (2.3), (2.4) with respect to q we obtain the equilibrium value of q:

$$q^2 = \delta/2\kappa \equiv q_0^2 \qquad \alpha_0 \equiv \delta^2/4\kappa = \kappa q_0^4 \tag{4.1}$$

where the notation α_0 is introduced, which is used in the following. Substituting (4.1) into (2.4), we obtain $\alpha(q_0) = \alpha - \alpha_0$. Minimizing now (2.3) with respect to ρ, we arrive at the expression

$$\Phi_{\mathrm{IC}} = -(\alpha - \alpha_0)^2/4\beta. \tag{4.2}$$

Minimizing potential (2.5) with respect to P_y we obtain

$$\Phi_{\mathrm{C}} = 0 \qquad \Phi_{0/1} = -3\alpha^2/8\beta. \tag{4.3}$$

Minimizing potentials (2.6) and (2.7) for the $C_{m/l}$ phases with respect to Q_1, Q_2, and φ, we obtain as a result for the possible phases c_1 and c_2 the solutions

$$\begin{aligned} &c_1\text{: } \cos 2l\varphi = 1,\ Q_1 = \pm(a_1/2\kappa_1)R^l,\ Q_2 = 0 \\ &c_2\text{: } \cos 2l\varphi = -1,\ Q_1 = 0,\ Q_2 = \pm(a_2/2\kappa_2)R^l \end{aligned} \tag{4.4}$$

provided that $\kappa_{1,2} > 0$. The phase c_3 can be neglected as explained above. Substituting (4.4) into (2.6) and (2.7), we arrive at the expressions

$$\Phi_{m/l} = \alpha(q_{m/l})R^2 + \beta R^4 - |\alpha'_{2l}|R^{2l} \qquad \alpha'_{2l} = \tilde{\alpha}'_{2l} + a_1^2/8\kappa_1 - a_2^2/8\kappa_2. \tag{4.5}$$

The phases c_1 and c_2 are stable at $\alpha'_{2l} > 0$, and $\alpha'_{2l} < 0$, respectively.

Minimizing (4.5) with respect to R and using the condition for weak anisotropy, we obtain

$$\Phi_{m/l} = -\frac{\alpha^2(q_{m/l})}{4\beta}\left[1 + \frac{|\alpha'_{2l}|}{\beta}\left(\frac{-\alpha(q_{m/l})}{2\beta}\right)^{l-2}\right]. \tag{4.6}$$

The condition for weak anisotropy consists in the fact that the anisotropic, i.e. φ-dependent, invariants in potential (2.6) are small in comparison with the isotropic invariant, which is independent of φ. As can be seen from (4.5) and (4.6), this condition has the form

$$\frac{|\alpha'_{2l}|R^{2l}}{2\beta R^4} = \frac{|\alpha'_{2l}|}{2\beta}\left(\frac{-\alpha(q_{m/l})}{2\beta}\right)^{l-2} \ll 1. \tag{4.7}$$

The larger l, the better (4.7) is fulfilled. For $l = 2$, condition (4.7) is not fulfilled. However, for $\Phi_{1/2}$ we can obtain an explicit expression neglecting this condition. It is not reproduced here, since in BCCD the $C_{1/2}$ phase is not observed.

Expressions (4.4)–(4.7) are obviously applicable to potentials (3.1)–(3.3), provided that the coefficients and variables are changed. However, the case of the phase c_1 for potential (3.3) requires additional consideration. In this case κ_1 has to be replaced by $\kappa_1 = \alpha + 4\beta R^2 = 2\alpha_0 - \alpha$, as follows from (3.3) under condition (4.7). This value is comparatively small. It is even possible to write out for the quantity $a_1^2/8\kappa_1$ a separate condition for weak anisotropy (different to (4.7)), but we shall not make use of this possibility, since the quantity a_1 has no independent meaning in the absence of the field F_1.

A phenomenological approach for accounting for the temperature sequence of phase transitions in BCCD was used in [12] (see also [13], where the P-dependence of the coefficients in the thermodynamic potential was taken into account). This approach differs from the one used in the present study and in [9] by the simplification of the term $\alpha'_{2l}R^{2l} = \beta_{eff}R^4$, where β_{eff} is assumed to be constant (we have replaced the notation of [12] and [13] by the notation used in this paper), and also by the use of the excess term $P_y^2(\partial P_y/\partial z)^2$ in (2.1), whereas the T- and P-dependences of the coefficient δ in (2.4) were not taken into consideration. However, although the presentation in [12, 13] is less rigorous, the approach is in essence close to the one presented in this paper and in [9] for the case where $E_y = 0$.

5. Boundaries between different phases

We now obtain expressions for the boundaries between the different phases by equating the thermodynamic potentials for these phases. We construct a phase diagram in the plane $\delta/2\kappa$, $(\alpha_0 - \alpha)/\kappa$, choosing these variables as coordinate axes. It is convenient to introduce the dimensionless variables

$$D \equiv \frac{\delta}{2\kappa} \qquad A \equiv \frac{\alpha_0 - \alpha}{\kappa} \qquad A_l \equiv \frac{\kappa}{2\beta}\left(\frac{|\alpha'_{2l}|}{\kappa}\right)^{1/(l-1)}. \tag{5.1}$$

The variables D and A have already been mentioned. We emphasize that each $C_{m/l}$ phase is characterized by only one dimensionless parameter A_l depending on the magnitude of the coefficient α'_{2l}.

The C–IC boundary, as follows from (4.2) and (4.3), has the form

$$A = 0. \tag{5.2}$$

For the C–$C_{0/1}$ boundary we obtain from (4.3) the expression ($D < 0$)

$$A = D^2. \tag{5.3}$$

The IC–$C_{0/1}$ boundary, as follows from (4.2) and (4.3), has the form

$$A = cD^2 \qquad c \equiv (1 - \sqrt{2/3})^{-1} \approx 5.45. \tag{5.4}$$

These three boundaries, equations (5.2)–(5.4), intersect at a single point, which is called the Lifshitz point (the L point) [7]. Its coordinates are

$$A = 0 \qquad D = 0. \tag{5.5}$$

For the IC–$C_{m/l}$ boundary we obtain from (4.2) and (4.6) the expression

$$A = \frac{1}{A_l}(D - q_{m/l}^2)^{2/(l-1)} \qquad \text{or} \qquad D = q_{m/l}^2 \pm (A_l A)^{(l-1)/2}. \tag{5.6}$$

The condition (4.7) for weak anisotropy is reduced using (5.6) to the form

$$(A_l A)^{l-1} A^{-1} \ll 1. \tag{5.7}$$

It is obvious from (5.6), and also from (5.7), that the greater $1/l$ and A_l are, the wider the area of existence of the $C_{m/l}$ phase is in the D–A diagram.

For the $C_{m/l}$–$C_{m'/l'}$ boundaries we obtain from (4.6) under condition (5.7) the expression

$$(D - q_{m/l}^2)^2 - (A_l A)^{l-1} = (D - q_{m'/l'})^2 - (A_{l'} A)^{l'-1} \tag{5.8}$$

which can be rearranged to give an expression for D:

$$D = (1/2)(q_{m/l}^2 + q_{m'/l'}^2) - (1/2)(q_{m/l}^2 - q_{m'/l'}^2)^{-1}[(A_l A)^{l-1} - (A_{l'} A)^{l'-1}]. \tag{5.9}$$

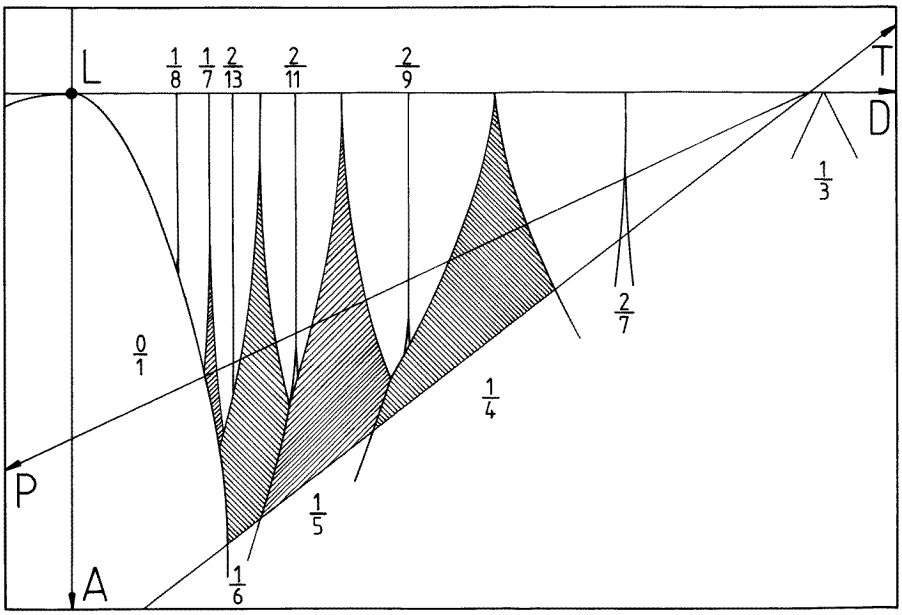

Figure 2. The D–A phase diagram.

Note that the boundaries IC–$C_{m/l}$, IC–$C_{m'/l'}$, equation (5.6), and $C_{m/l}$–$C_{m'/l'}$, equation (5.8), intersect at a single point, as they should.

For the $C_{0/1}$–$C_{m/l}$ boundary we obtain from (4.3) and (4.6) under condition (5.7) the expression

$$A = cD^2 - (c-1)[(D - q_{m/l}^2)^2 - (A_l A)^{l-1}] \tag{5.10}$$

which can be rearranged to give an expression for D. Usually this boundary differs slightly from the IC–$C_{0/1}$ boundary; see (5.4). The boundaries IC–$C_{0/1}$, equation (5.4), IC–$C_{m/l}$, equation (5.6), and $C_{0/1}$–$C_{m/l}$, equation (5.10), intersect at a single point. This is also the case for the boundaries $C_{m/l}$–$C_{m'/l'}$, equation (5.8), $C_{0/1}$–$C_{m/l}$, equation (5.10), and $C_{0/1}$–$C_{m'/l'}$, equation (5.10). The intersection of these boundaries and also of those mentioned above at a single point confirms the fact that none of the expressions for the boundaries contain terms which are beyond the accuracy of the approach determined by condition (5.7).

6. Phase diagrams

In order to construct the D–A diagram for BCCD, we must choose values of the parameters A_l for each $C_{m/l}$ phase. In practice, such a choice must be realized via a best fit of the theoretical T–P diagram, as obtained from the D–A diagram, to the experimental T–P diagram shown in figure 1. We choose the following values of the parameters†:

$$\begin{aligned} &A_3 = 10 \qquad A_4 = 30 \qquad A_5 = 40 \qquad A_6 = A_7 = A_8 = 50 \\ &A_7 = A_9 = 80 \qquad A_{11} = A_{13} = 100 \end{aligned} \tag{6.1}$$

for the $C_{m/l}$ phases with $q_{m/l} = m/l = 1/3, 1/4, 1/5, 1/6, 1/7, 1/8; 2/7, 2/9, 2/11, 2/13$, respectively (other $C_{m/l}$ phases are omitted from our consideration). Even with such a crude

† A_7 occurs twice, since there exist two phases with $l = 7$.

choice of A_l-values (with accuracy only up to the first digit), we obtain a rather satisfying agreement between the theoretical and experimental T–P diagrams (see below).

Figure 2 shows the D–A phase diagram constructed according to the expressions (5.1)–(5.10) and (6.1). The $C_{m/l}$ phases are hatched in figure 2 and labelled with their ratios m/l. L denotes the L point with its coordinates given by (5.5). Note that A_l-values different from those in (6.1) were chosen, and the corresponding D–A diagram was constructed in [15] in order to explain the sequence of C, IC, and $C_{m/l}$ phases in the experimental T-diagram given in [14].

The two coefficients α and δ of the thermodynamic potentials are anomalously small, and hence their dependence on T and P is crucial. The remaining coefficients $\beta, \kappa, \alpha'_{2l}$ have, generally speaking, a normal magnitude, i.e. they can be considered as constants, independent of T and P (and, for the same reasons, independent of q). We assume that α and δ and hence A and D (see (4.1) and (5.1)) depend linearly on T and P. This means that the axes T and P in figure 2 are straight lines. Their position, orientation, and scale are determined from the best fit to the experimental T–P diagram.

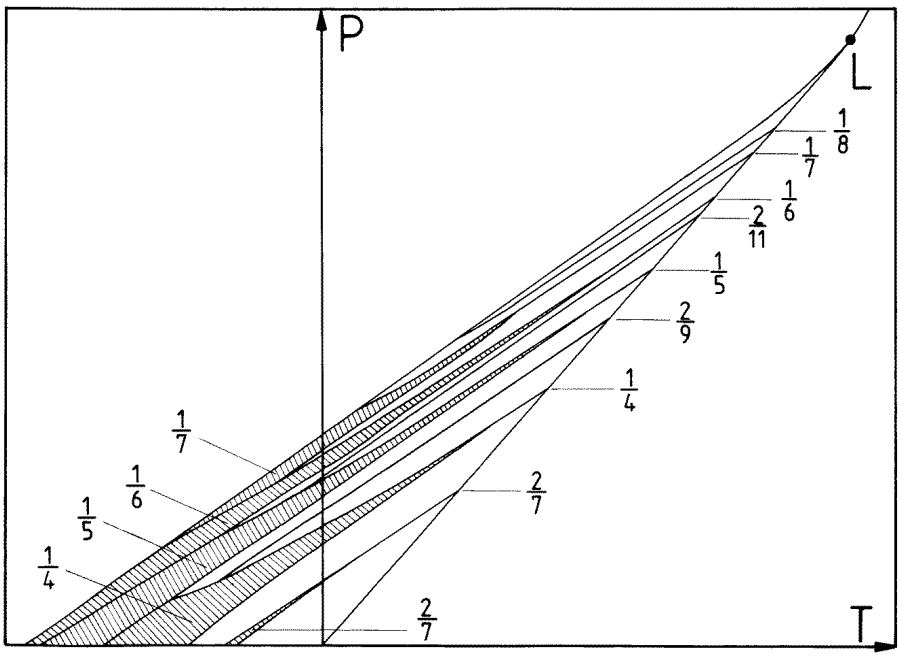

Figure 3. The theoretical T–P phase diagram for BCCD. The $C_{m/l}$ phases with $m/l = 2/7, 1/4, 1/5, 1/6$, and $1/7$ are hatched as in figure 2; L labels the L point.

The orientation of the T-axis in the D–A diagram in figure 2 is chosen in such a way that the $C_{m/l}$ phases intersected by the T-axis are the same and have approximately the same widths as in figure 1 (at $P = 0$). The scale of the T-axis in figure 2 is chosen in such a way that we obtain the correct temperature interval between the C–IC and $C_{0/1}$–$C_{1/6}$ transitions, as given in figure 1. The orientation and scale of the P-axis has been chosen accordingly. Using these choices for the T- and P-axes, we replot the D–A diagram of figure 2 in the T, P-plane. The resulting theoretical T–P phase diagram is shown in figure 3.

By comparing figure 3 with figure 1 we see that the theoretical and experimental T–P phase diagrams agree sufficiently well. This agreement can be improved by making a more

suitable selection of A_l-values, or by achieving a more precise orientation of the T- and P-axes in the D–A phase diagram. We shall not follow this procedure in this study, partly because of some scatter in the experimental data (see, e.g., tables given in [12] and in [14]). In general, the coefficients of the thermodynamic potentials can be determined from such fitting procedures.

7. Conclusions

In conclusion, we have returned to discussing the approximations and assumptions which were made when constructing the theoretical D–A and T–P phase diagrams. The single-harmonic approximation was used for the IC phase. This leads to insignificant errors when determining the boundaries between the IC and $C_{m/l}$ phases.

A weak-anisotropy condition was used for the $C_{m/l}$ phases, thus allowing us to obtain explicit expressions for the potentials and hence for the boundaries of the $C_{m/l}$ phases. However, for small l and in regions of large A-values in the D–A diagram, this condition is not well satisfied.

The variables D and A were assumed to be linearly dependent on T and P, while the A_l were assumed to be constant. However, these assumptions are less well fulfilled for wide T- and P-intervals.

The approximations and assumptions given above and used to construct theoretical phase diagrams did not prevent us from obtaining a fairly good agreement between the theoretical and experimental T–P phase diagrams for BCCD. This demonstrates that the phenomenological approach to structural phase transitions, which was always well justified, also happens to be an adequate description in cases of complicated phase diagrams, where, in addition to the initial phase, the incommensurate and a large number of commensurate phases occur.

Acknowledgment

One of the authors (DGS) gratefully acknowledges the financial support of the Deutsche Forschungsgemeinschaft.

References

[1] Ao R, Schaack G, Schmitt M and Zöller M 1989 *Phys. Rev. Lett.* **62** 183
[2] Schaack G 1990 *Ferroelectrics* **104** 147
[3] le Maire M, Lingg G, Schaack G, Schmitt-Lewen M and Strauß G 1992 *Ferroelectrics* **125** 87
[4] Illing M, Schaack G and Schmitt-Lewen M 1994 *Ferroelectrics* **155** 341
[5] Kityk A V, Soprunyuk V P, Vlokh O G, Sveleba S A and Czapla Z 1993 *J. Phys.: Condens. Matter* **5** 7415
[6] Chaves M R, Kiat J M, Schwarz W, Schneck J, Almeida A, Klöpperpieper A, Müser H E and Albers J 1993 *Phys. Rev.* B **48** 5852
[7] Hornreich R M, Luban M and Shtrikman S 1975 *Phys. Rev. Lett.* **35** 1678
[8] Michelson A 1977 *Phys. Rev.* B **16** 577
Michelson A 1977 *Phys. Rev.* B **16** 593
[9] Sannikov D G 1989 *Zh. Eksp. Teor. Fiz.* **96** 2197 (Engl. Transl. 1989 *Sov. Phys.–JETP* **69** 1244)
Sannikov D G 1990 *Zh. Eksp. Teor. Fiz.* **97** 2024 (Engl. Transl. 1990 *Sov. Phys.–JETP* **70** 1144)
[10] Pérez-Mato J M 1988 *Solid State Commun.* **67** 1145
[11] Sannikov D G 1991 *Kristallografiya* **36** 813 (Engl. Transl. 1991 *Sov. Phys.–Crystallogr.* **36** 455)
[12] Ribeiro J L, Tolédano J C, Chaves M R, Almeida A, Müser H E, Albers J and Klöpperpieper A 1990 *Phys. Rev.* B **41** 2343

[13] Chaves M R, Almeida A, Kiat J M, Tolédano J C, Schneck J, Glass R, Schwarz W, Ribeiro J L, Klöpperpieper A and Albers J 1995 *Phys. Status Solidi* b **189** 97
[14] Unruh H-G, Hero F and Dvořák V 1989 *Solid State Commun.* **70** 403
[15] Sannikov D G 1991 *Ferroelectrics* **124** 49